

Can We Trust LLMs on Memristors? Diving into Reasoning Ability under Non-Ideality

Taiqiang Wu^{†1}, Yuxin Cheng^{†1}, Chenchen Ding^{†1},
Runming Yang¹, Xincheng Feng¹, Wenyong Zhou¹, Zhengwu Liu^{*1}, Ngai Wong^{*1}
¹The University of Hong Kong [†]Equal contributions. ^{*}Corresponding authors. takiwu@connect.hku.hk

Abstract

Memristor-based analog compute-in-memory (CIM) architectures provide a promising substrate for the efficient deployment of Large Language Models (LLMs), owing to superior energy efficiency and computational density. However, these architectures suffer from precision issues caused by intrinsic non-idealities of memristors. In this paper, we first conduct a comprehensive investigation into the impact of such typical non-idealities on LLM reasoning. Empirical results indicate that reasoning capability decreases significantly but varies for distinct benchmarks. Subsequently, we systematically appraise three training-free strategies, including thinking mode, in-context learning, and module redundancy. We thus summarize valuable guidelines, i.e., shallow layer redundancy is particularly effective for improving robustness, thinking mode performs better under low noise levels but degrades at higher noise, and in-context learning reduces output length with a slight performance trade-off. Our findings offer new insights into LLM reasoning under non-ideality and practical strategies to improve robustness.

CCS Concepts

- **Computing methodologies** → **Natural language generation;**
- **Hardware** → *Hardware reliability.*

Keywords

LLM, Memristor Non-Ideality, Reasoning, Robustness

ACM Reference Format:

Taiqiang Wu^{†1}, Yuxin Cheng^{†1}, Chenchen Ding^{†1}, Runming Yang¹, Xincheng Feng¹, Wenyong Zhou¹, Zhengwu Liu^{†1}, Ngai Wong^{*1}. 2025. Can We Trust LLMs on Memristors? Diving into Reasoning Ability under Non-Ideality. In *Proceedings of DAC: The Chips to Systems Conference (DAC 2026)*. ACM, New York, NY, USA, 8 pages. <https://doi.org/XXXXXXX.XXXXXXX>

1 Introduction

Large language models (LLMs), such as GPT-4 [1], Llama [12], and Qwen [35], have demonstrated promising performance in Natural Language Processing (NLP) tasks, attributed to the superior reasoning capability [15]. However, this success, primarily driven by the massive model parameters and scaled chain-of-thought (CoT)

outputs, also presents challenges for practical deployments, such as high energy cost [4, 32].

For efficient deployment of neural network, one promising approach is to leverage analog compute-in-memory (CIM) architectures with memristors such as resistive random-access memory (RRAM) [36], which perform computations directly within memory arrays to achieve high energy efficiency and high computational density [21]. By eliminating the energy-intensive data movement between memory and processing units, a key bottleneck in traditional computation system based on von Neumann architectures, CIM architectures are particularly well-suited for the matrix-vector multiplications that dominate LLM inference.

This approach has also attracted increasing research attention for LLM deployment in recent years. For instance, deploying Llama 3 1B and 3B on RRAM-based CIM saves more than 40× energy compared to GPU implementations [32]. However, despite its energy efficiency, memristor-based CIM suffers from inherent non-ideality issues, i.e., introducing noise during the calculation process. As shown in Figure 1, this inherent non-ideality manifests as extra block-wise Gaussian noise and stuck-at faults in the weights. Hence, this raises an intriguing question: *How does such non-ideality impact the reasoning capability of LLMs? If so, can we eliminate or attenuate this side effect?*

In this paper, we conduct a comprehensive investigation into the impact of non-ideality in memristor-based analog CIM on LLM reasoning using RRAM-based CIM as an example. Without loss of generality, we simulate multi-level non-ideality and then evaluate on three selected benchmarks: IFEval [39], GPQA-Diamond [25], and MATH-500 [22]. Empirical results indicate that very slight noise ($\sigma = 0.005$) can *occasionally* lead to better results [32], while greater noise leads to severe performance degradation and greater variance. In particular, the mathematical reasoning performance decreases rapidly, since they typically require multi-step reasoning and thus are more fragile to perturbations [33]. Meanwhile, the output tokens increase exponentially. High noise would lead to excessively long outputs, nullifying the primary advantage of memristors.

To address this issue, re-training the LLMs is often unaffordable, as LLMs require huge amounts of data and thousands, or even millions, of GPU days [15, 35]. Hence, we systematically appraise three *training-free* strategies to eliminate or attenuate the side effects of such non-ideality, including thinking mode, in-context learning (ICL, [11]), and module redundancy [34]. The thinking mode performs better under relatively low noise levels, but its efficacy diminishes at larger noise levels due to the collapse of the thinking mode. ICL, by providing examples within the input, effectively reduces output length thanks to the provided extra solution patterns, but also suffers from a slight performance drop and increased input

Permission to make digital or hard copies of all or part of this work for personal or classroom use is granted without fee provided that copies are not made or distributed for profit or commercial advantage and that copies bear this notice and the full citation on the first page. Copyrights for components of this work owned by others than the author(s) must be honored. Abstracting with credit is permitted. To copy otherwise, or republish, to post on servers or to redistribute to lists, requires prior specific permission and/or a fee. Request permissions from permissions@acm.org.

DAC 2026, Long Beach, CA

© 2025 Copyright held by the owner/author(s). Publication rights licensed to ACM.
ACM ISBN 978-1-4503-XXXX-X/2018/06
<https://doi.org/XXXXXXX.XXXXXXX>

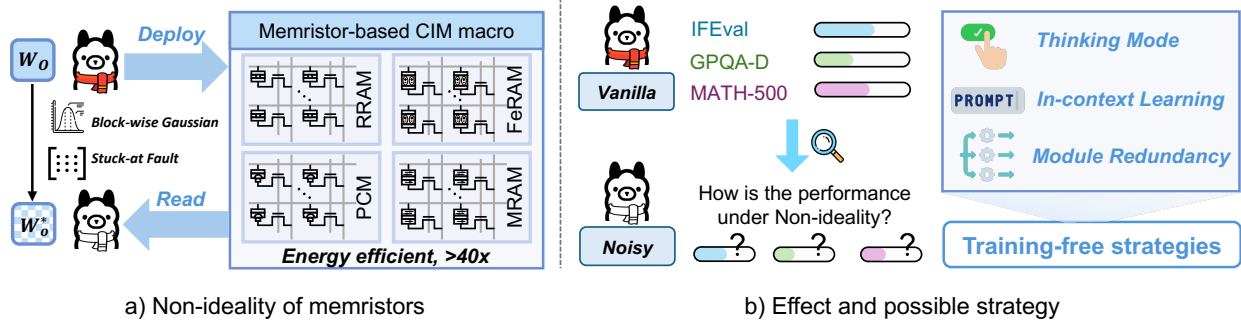


Figure 1: Overview of the non-ideality when deploying LLM on memristor-based analog CIM architectures. In this paper, we study the impact on LLM reasoning and discuss available training-free solutions.

length. For the module redundancy strategy, we find that greater redundancy generally improves robustness, and that shallow layers are particularly vital. Based on these observations, we summarize practical guidelines including the behaviors and applicable scenarios. In addition, we conduct experiments on more LLMs (Qwen3 1.7B and Llama 3.2 1B) to demonstrate the effectiveness and robustness.

Our contributions can be summarized as follows:

- We conduct a comprehensive investigation into the impact of memristor non-ideality on LLM reasoning, highlighting an important and non-negligible issue for practical deployment.
- We systematically appraise various training-free strategies to attenuate the impact of such non-ideality, and provide valuable insights into their mechanisms.
- We conduct extensive experiments on the Qwen3 and Llama series, and summarize practical guidelines for distinct scenarios.

2 Related Work

LLMs benefit from a consistently scaled reasoning trajectory [15, 31], driving rapid and significant advancements and enabling them to achieve state-of-the-art performance across various domains [2, 17]. With training for articulating long reasoning steps, the power of LLM is rapidly expanded to advanced mathematics [18], code generation [37], logical reasoning [3, 6], and autonomous planning applications [14]. However, the substantial computational overhead associated with reasoning hinders the deployment and further application of advanced LLMs in edge computing [13, 29].

Consequently, research on integrating novel computing components, such as Memristors [30], to optimize and adapt LLM has become increasingly important [28, 32]. Meanwhile, memristors achieve high energy efficiency but also suffer from non-ideality due to the stochastic nature of the switching process [8, 19]. Previous works have studied the impact of non-ideality toward LLM finetuning [32] and classification task via BERT [26, 30].

In this paper, we are the first to discuss the advanced LLM reasoning under non-ideality and discuss available training-free strategies.

3 Reasoning Under Non-Ideality

3.1 Non-Ideality Simulation

During inference, memristor non-ideality primarily manifests as random noise from device-to-device and cycle-to-cycle variability [24]. Without loss of generality, we implement simulation for both *block-wise* Gaussian noise and stuck-at faults.

Block-wise Gaussian Noise. This model introduces noise to the weights of individual memristor sub-blocks (tiles). For a target memristor tile of shape $m \times n$, we partition the larger weight matrix $\mathbf{W}_0 \in \mathbb{R}^{d_1 \times d_2}$ into smaller blocks. The non-ideality simulation is then formulated as:

$$\{\mathbf{W}_{0,[i,j]}\}_{i=1,j=1}^{k,t} = \text{Split}(\mathbf{W}_0), \text{ where } k = \lceil \frac{d_1}{m} \rceil, t = \lceil \frac{d_2}{n} \rceil, \quad (1)$$

$$\mathbf{W}_0^* = \text{Cat}(\{\mathbf{W}_{0,[i,j]} + \mathbf{N}_{[i,j]} \cdot \max(|\mathbf{W}_{0,[i,j]}|)\}_{i=1,j=1}^{k,t}) \quad (2)$$

$$\mathbf{N}_{[i,j]} \sim \mathcal{N}(0, \sigma^2 \mathbf{I}) \quad (3)$$

where $\text{Split}(\cdot)$ and $\text{Cat}(\cdot)$ denote the matrix splitting and concatenation operations. $\mathbf{W}_{0,[i,j]}$ is the partitioned weight block, and \mathbf{W}_0^* is the resultant noise-injected weight matrix. $\mathbf{N}_{[i,j]}$ is a noise matrix where each element is drawn from a Gaussian distribution with zero mean and variance σ^2 . The noise is scaled by the maximum absolute value of the block, and σ represents the noise level, with a larger value denoting stronger noise.

Stuck-at Faults. Stuck-at Faults (SAFs) are physical defects where a memory cell becomes permanently stuck in either a high resistance state (HRS) or a low resistance state (LRS). In this paper, we simulate the effect of SAFs by introducing random bit-flips to the mantissa of the bf16 weight values [7]. We model this as a probabilistic event: for each of the 7 bits in the mantissa, there is a probability p that it will be flipped (0→1 or 1→0). This parameter p represents the SAF rate in the memristor array. For example, consider the value 0.028:

$$0.028 = 0011110011100101 \quad (4)$$

If two bits happened to flip, then one possible outcome is:

$$0.029541015625 = \underbrace{0}_{\text{Sign}} \underbrace{01111001}_{\text{Exponent}} \underbrace{1110001}_{\text{Flipped Mantissa}} \cdot \quad (5)$$

Then the read value is different from the input value.

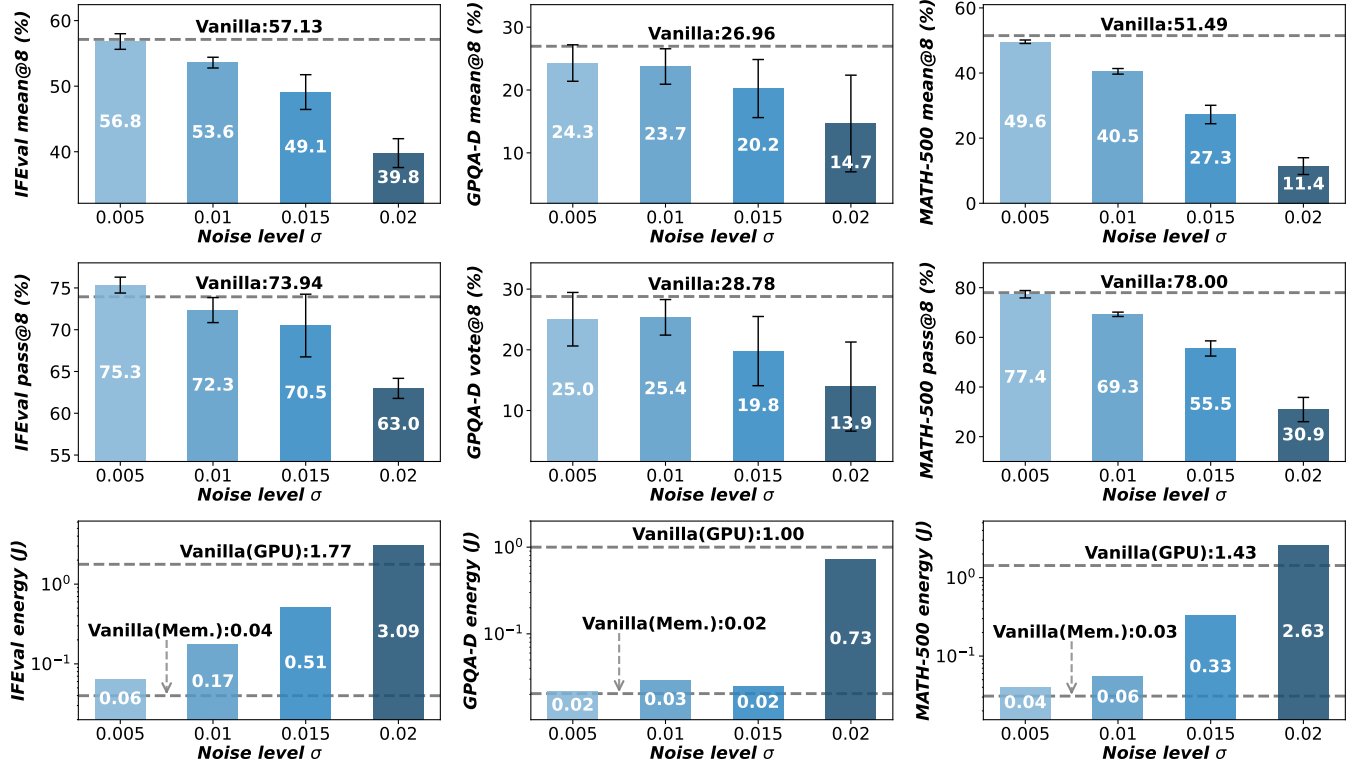


Figure 2: Performance of Qwen3 0.6B under Non-ideality at various noise levels σ . The SAF ratio p is 0.01. A darker color denotes larger noise. We report the results on IFEval, GPQA-D, and MATH-500. The vanilla performance is indicated by the dotted line.

Energy and Area Simulation. We assume that static vector-matrix multiplications are performed by memristor-based analog CIM (with RRAM used as the example). Non-parametric operations like Softmax and activation operation are set to be computed in digital region. With this assumption, we developed a simulation system for energy and area estimation with RRAM-based analog CIM following the general practices in literature [23, 36]. The energy consumption and area of analog CIM macros is evaluated with XPESim [38], and the digital region operations are evaluated with literature reported data [27].

3.2 Experimental Setup

Our primary experiments are conducted on Qwen3 0.6B [35]. Results on additional LLMs are presented in Section 4.4. To simulate memristor non-ideality, we set the block size $m \times n$ to 64×64 and evaluate noise levels $\sigma \in \{0.005, 0.01, 0.015, 0.02\}$ following Wu et al. [32]. For the Stuck-at Fault (SAF) simulation, the bit-flip probability p is set to 0.01. Under each noise configuration, we repeat 5 independent runs and report the mean score along with the standard deviation.

We evaluate performance on three prominent reasoning benchmarks: 1) IFEval [39] for instruction-following ability; 2) GPQA-Diamond (GPQA-D [25]) for scientific reasoning ability using challenging multiple-choice questions from biology, physics, and chemistry; and 3) MATH-500 [22] for mathematical reasoning using 500

uniformly selected test problems. All benchmarks are evaluated in a zero-shot setting. Besides the average accuracy (Mean@8), we further report the Pass@8/Vote@8 and energy costs. During generation, we follow the official guidelines for sampling parameters: temperature $t = 0.7$, Top-p = 0.8, and Top-k = 20. The maximum output length is set to 32k tokens, and we sample 8 responses for each prompt. Evaluations are conducted on 8 NVIDIA H200 GPUs using the Opencompass framework [10].

3.3 Main Results

Figure 2 reports the main results on Qwen3 0.6B. We can draw several key observations as follows.

Reasoning capability degrades under non-ideality, and instability increases with stronger noise. There is a strong negative correlation between the noise level σ and reasoning performance. As σ increases from 0.005 to 0.02, performance on all six metrics degrades. Furthermore, the standard deviation, visualized by the error bars, visibly increases with higher noise levels.

Slight noise can sometimes lead to better performance. We observe a nuanced effect at the lowest noise level. While most metrics are immediately degraded, the performance for IFEval Pass@8 at $\sigma = 0.005$ (75.3%) is slightly *higher* than the ideal baseline (73.94%). This observation is consistent with the findings of Wu et al. [32], suggesting that a minimal level of noise can sometimes act as a regularizer, potentially improving performance on specific tasks.

However, this minor benefit is selective and is quickly overwhelmed by the detrimental effects of noise, especially on MATH-500.

Among these tasks, mathematical reasoning suffers most. Another key finding is that the impact of noise is highly task-dependent. For mathematical reasoning (MATH-500), performance is extremely sensitive, with Pass@8 plummeting from 77.4% down to 30.9%. This strongly suggests that tasks requiring high-precision, multi-step logical deduction are fundamentally more vulnerable to the weight perturbations caused by memristor non-ideality.

The energy cost explodes under high noise, nullifying the primary advantage of memristor. The deployment on memristor is exceptionally energy-efficient, consuming only 0.03J on MATH-500 compared to the 1.43J of the GPU. However, this energy cost rises exponentially with the noise level, ballooning from 0.04J at $\sigma = 0.005$ to a staggering 2.63J at $\sigma = 0.02$. Critically, this 2.63J consumption at high noise is significantly worse than the 1.43J required by the standard GPU implementation, due to the excessively long and unstructured outputs. Consequently, the intrinsic energy benefits of memristor are completely negated in high-noise scenarios.

3.4 Error Analysis

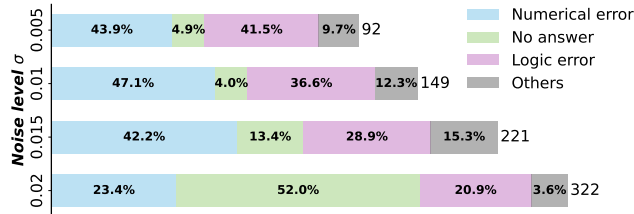


Figure 3: Error analysis of Qwen3 0.6B on Math-500. Larger noise leads to more formatting issues.

We further analyze the answers from MATH-500 with $\sigma = 0.02$ and employ Claude 4.5 to recognize the errors introduced by non-ideality. The errors are categorized into four main types: 1) *Numerical Error* for calculating process error; 2) *No Answer* that fails to generate the final answer; 3) *Logic Error* where the reasoning process is coherent but flawed; and 4) *Others* for all other failure modes, such as formatting issues or incoherent text. As shown in Figure 3, we observe that *No Answer* increases as the noise becomes stronger. The output reasoning trajectories mess up and fail to generate the final answer. This suggests that as non-ideality worsens, the fundamental ability to adhere to the requested task structure collapses.

3.5 Ablation on SAF ratio

Moreover, we conduct an ablation study on the SAF ratio p . As shown in Table 1, performance under the SAF only ($p = 0.001$) setting (e.g., 57.0 on IFEval, 51.6 on MATH-500) remains close to the Vanilla baseline (57.1 on IFEval, 51.5 on MATH-500). The larger the SAF ratio p , the worse the performance. Typical value for the SAF ratio is about 0.005 [16]. Therefore, we fix p to the highest typical value 0.01 in the following experiments.

Table 1: Ablation of SAF ratio p .

Noise	IFEval Mean@8 \uparrow	GPQA-D Mean@8 \uparrow	MATH-500 Mean@8 \uparrow
Vanilla	57.1	27.0	51.5
SAF ($p = 0.0005$)	57.0 \pm 0.4	26.6 \pm 1.1	51.5 \pm 0.3
SAF ($p = 0.001$)	57.0 \pm 0.4	26.7 \pm 1.2	51.6 \pm 0.6
SAF ($p = 0.0025$)	56.4 \pm 0.9	26.7 \pm 0.7	50.9 \pm 1.0
SAF ($p = 0.005$)	56.8 \pm 0.4	25.4 \pm 1.5	50.5 \pm 0.9
SAF ($p = 0.01$)	55.7 \pm 0.7	26.1 \pm 1.4	47.5 \pm 1.5

4 Extensive Analysis

4.1 Thinking Mode

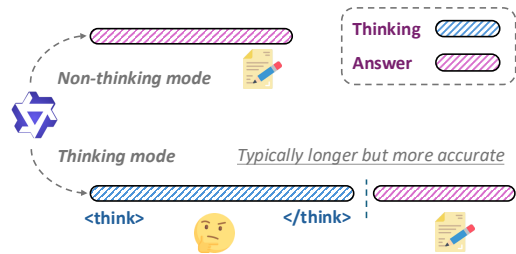


Figure 4: Comparison between Non-thinking and Thinking mode that introduces an explicit thinking process.

As shown in Figure 4, the thinking mode, encourages the LLMs to explicitly output the thinking process before finalizing the answers. Typically, the thinking mode outputs longer but more accurate responses. Therefore, on the thinking mode of Qwen3 models and set the hyperparameters accordingly: temperature $t = 0.8$, Top-p = 0.95. Moreover, we report the token ratio of the Thinking parts among the outputs.

Figure 5 indicates the results of the MATH-500 benchmark on Qwen3 0.6B across the full range of noise levels. These results reveal that the effectiveness of the thinking mode is highly dependent on the noise level. At relatively low noise levels ($\sigma \leq 0.01$), the thinking mode provides a significant robustness advantage over the vanilla baseline. However, for a larger noise level, the benefit of the thinking mode rapidly diminishes. This failure is directly related to a mode collapse, as indicated by the thinking ratio plummeting to near-zero at $\sigma = 0.02$. Specifically, LLMs generate lots of `<think></think>` and repeat some phrases, such as `Therefore, the final answer is: xxx Therefore, the final answer is: xxx`. It indicates that LLM fails to adhere to the explicit reasoning format and instead generates much longer but unstructured and repeated responses.

Practical Guidelines. Based on the observations, we recommend the thinking mode as a viable training-free strategy only when the non-ideality is well-controlled ($\sigma \leq 0.01$). However, practitioners should be aware of two critical limitations. First, the thinking mode incurs substantial computational overhead, generating 5-18 \times more output tokens than the vanilla model, leading to significantly higher inference latency and energy consumption on CIM architectures. Second, the mode collapse phenomenon at high noise

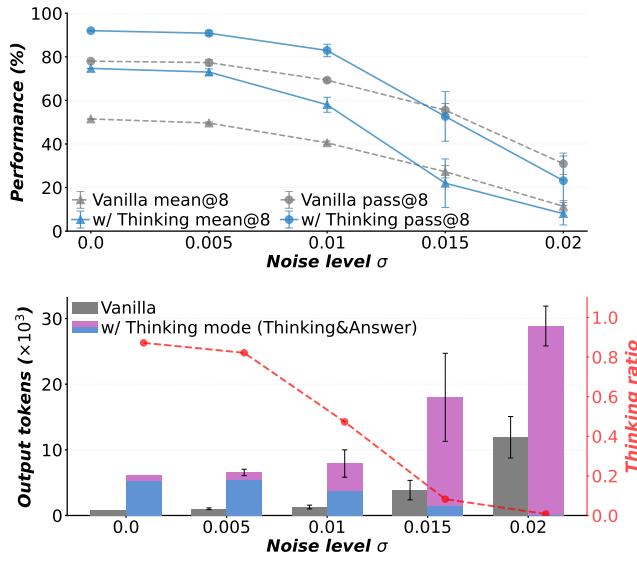


Figure 5: Comparison of Thinking and Non-thinking modes on MATH-500. The SAF ratio p is 0.01. We also report the token ratio of Thinking parts.

levels ($\sigma > 0.015$) renders this strategy not only ineffective but potentially harmful, as the model produces verbose yet unstructured outputs without meaningful reasoning.

4.2 In-context Learning

Question

Find the domain of the expression $\frac{\sqrt{x-2}}{\sqrt{5-x}}$. Please reason step by step, and put your final answer within `\boxed{}`.

We are given the expression: $\frac{\sqrt{x-2}}{\sqrt{5-x}}$. We are to find its domain — that is, all real values of x for which the expression is defined and real.

Step 1: Consider the square roots in the numerator and denominator ...

Step 2: Combine the inequalities ...

Step 3: Conclusion ...

Final Answer: `\boxed{\{2, 5\}}`

Solution

Figure 6: One example with a step-by-step solution under the in-context learning setting. We omit the details with ellipses.

Another strategy is in-context learning (ICL), where LLM learns from a few examples in the context without updating the parameters [11]. To obtain high-quality examples, we adapt Qwen3-Max thinking to answer the given questions. As shown in Figure 6, the response is well-organized and contains step-by-step solutions. Since the answer is quite long, we employ the 2-shot setting to include two examples.

Figure 7 indicates the detailed performance on MATH-500 for Qwen3 0.6B. We observe that ICL consistently underperforms the vanilla model across all noise levels for both Mean@8 and Pass@8

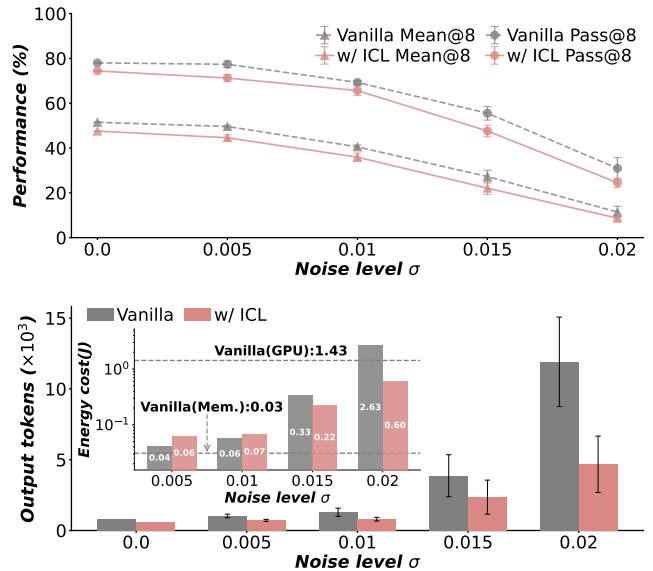


Figure 7: Performance on MATH-500 with and without in-context learning (2-shots). The SAF ratio p is 0.01. ICL effectively decreases the length of output tokens but also introduces longer input.

metrics. Meanwhile, ICL effectively decreases the length of output tokens compared to the exponential increase in the vanilla model. However, ICL also requires longer inputs to provide the in-context examples, which introduces a critical trade-off. Therefore, the total energy consumption is not always lower. At low-to-moderate noise levels (e.g., $\sigma \leq 0.015$), the energy cost of ICL is comparable to or even slightly higher than the vanilla RRAM baseline. The energy benefit of ICL only becomes apparent at very high noise levels ($\sigma = 0.02$), where it curtails the catastrophic token generation, resulting in significantly lower energy consumption (0.60J vs. 2.63J) at the cost of slightly lower accuracy.

Practical Guidelines. ICL consistently leads to a degradation in reasoning accuracy (both Mean@8 and Pass@8) across all noise levels. At high noise levels, it acts as a safeguard against catastrophic energy consumption by enforcing a more structured and shorter output. However, in low-noise regimes, the longer input prompts required by ICL lead to slightly higher energy consumption while still delivering lower performance than the vanilla baseline. Future work could explore identifying more effective in-context examples to potentially improve robustness without this accuracy trade-off.

4.3 Module Redundancy

Another strategy is the module redundancy, aiming to reduce the noise level by repeating modules and calculating the average. We investigate this by repeating the Attention and FFN modules, as well as entire blocks of layers, under a high noise condition ($\sigma = 0.02$).

As shown in Table 2, repeating core components like FFN and Attention yields significant benefits. We observe that FFN redundancy is particularly effective. The FFN ($\times 4$) strategy, which quadruples the FFN modules, achieves the best performance in this category,

Table 2: Performance (5 runs) of Qwen3 0.6B without and with module redundancy strategies. The Energy is calculated on the MATH-500 task. For the noise simulation, σ is 0.02 and p is 0.01. Green denotes the best results, while blue for the second.

Method	Area (mm ²) ↓	Energy (J) ↓	IFEval		GPQA-D		MATH-500	
			Mean@8 ↑	Pass@8 ↑	Mean@8 ↑	Vote@8 ↑	Mean@8 ↑	Pass@8 ↑
Vanilla (GPU)	806	1.43	57.1±0.6	74.1±0.3	27.0±1.9	30.3±2.1	51.5±1.6	78.4±0.6
Vanilla (Memristor $\sigma=0.02$)	75	2.63	39.8±2.2	63.0±1.2	14.7±7.7	13.9±7.3	11.4±2.6	30.9±4.9
<i>Module Redundancy</i>								
Attention (×2)	103	1.81	46.0±3.8	70.5±3.2	20.4±5.4	19.8±6.1	18.6±2.9	41.3±3.8
Attention (×4)	160	0.45	48.3±0.9	70.6±3.2	20.7±6.0	21.4±6.1	25.1±2.8	51.9±3.6
FFN (×2)	114	0.69	49.6±3.4	70.7±3.2	18.4±9.0	18.3±9.9	21.6±2.5	47.6±3.2
FFN (×4)	193	0.22	52.2±1.9	73.2±1.7	20.4±3.5	19.2±3.7	30.1±2.2	58.7±2.1
<i>Layer Redundancy</i>								
Layer 0-6 (×2)	91	1.94	45.1±3.7	67.4±2.5	14.8±3.6	13.8±4.8	17.7±0.9	39.0±0.6
Layer 7-13 (×2)	91	1.79	44.7±0.4	69.7±1.3	16.6±7.9	16.6±9.0	13.1±4.1	34.0±8.0
Layer 14-20 (×2)	91	1.20	44.4±3.3	68.7±2.2	16.6±5.0	16.2±5.1	15.2±1.3	36.7±3.4
Layer 21-27 (×2)	91	4.58	42.2±5.6	65.2±5.9	10.0±7.4	8.9±7.5	10.9±2.7	28.1±4.7

restoring the MATH-500 Mean@8 score from a baseline of 11.4 to 30.1 and Pass@8 from 30.9 to 58.7. It also leads the IFEval recovery (52.2 for Mean@8). Attention (×4) also provides a strong boost, securing the second-best results on MATH-500 (25.1 for Mean@8). Crucially, this approach can also be exceptionally energy-efficient. While the noisy baseline consumes 2.63J, the FFN (×4) strategy cuts this to just 0.22J, and Attention (×4) to 0.45J. Both are far more efficient than the original GPU implementation (1.43 J), demonstrating that module redundancy can simultaneously recover reasoning performance and restore the energy advantage of memristor.

We also explored repeating entire layers. There are 28 layers in Qwen3 0.6B, and we repeat every 8 layers. The results indicate that the early layers are most vital. Repeating the first 7 layers (Layer 0-6) provides a noticeable boost to MATH-500 performance (17.7 for Mean@8). However, repeating deeper layers is less effective or even detrimental; repeating the final layers (Layer 21-27) results in catastrophic energy consumption (4.58J) and poor performance. This suggests that robustness is highly dependent on the shallow or early layers of the model.

Practical Guidelines. Based on the results in Table 2, a clear trade-off emerges between performance, energy, and area. The observations suggest a targeted strategy applying heavy module redundancy only to the critical shallow layers. This approach provides the most practical trade-off, capturing the significant performance and energy-efficiency gains observed in the 4× module tests while avoiding the prohibitive area cost of applying them to the entire model. This targeted method also avoids the severe performance and energy degradation seen when repeating deeper layers.

4.4 Results on More LLMs

We further conduct the experiments on Qwen3 1.7B and Llama 3.2 1B models. Based on the guidelines, we try a simple strategy to repeat 4 times for the first 1/4 of the total layers, denoted as Shallow (4×). The decoding hyperparameters are set following official guidelines. For the noise simulation, the σ is 0.02.

Table 3: Performance on Llama 3.2 1B and Qwen3 1.7B.

Method	IFEval	GPQA-D	MATH-500	Energy	Area
	Mean@8 ↑	Mean@8 ↑	Mean@8 ↑	(J) ↓	(mm ²) ↓
Llama 3.2 1B					
Vanilla (GPU)	50.0	23.2	15.8	12.0	806
Vanilla ($\sigma = 0.02$)	39.9	17.4	7.6	1.5	121.3
Shallow (4×)	47.4	18.7	8.5	0.7	207.1
Qwen3 1.7B					
Vanilla (GPU)	67.1	29.9	74.0	4.6	806
Vanilla ($\sigma = 0.02$)	40.9	10.5	19.0	7.2	174.3
Shallow (4×)	59.9	26.7	53.8	0.3	299.9

Table 3 reports the benchmark performance and energy on MATH-500. The results clearly demonstrate that Shallow (4×) effectively achieves a good balance between performance and efficiency. For Qwen3 1.7B, it recovers the MATH-500 score to 53.8 and IFEval to 59.9, closing a significant portion of the performance gap. Most importantly, it does so while being exceptionally energy-efficient, cutting the energy cost from 7.2J down to a mere 0.3J. The same trend holds for Llama 3.2 1B, where performance is recovered across all benchmarks (e.g., MATH-500 from 7.6 to 8.5) and energy is halved from 1.5J to 0.7J. In summary, our guidelines are practical and applicable to other LLMs, demonstrating their effectiveness and robustness.

5 Conclusion

In this paper, we conducted a comprehensive investigation into the impact of non-ideality on LLM reasoning. Our findings reveal that reasoning capability, particularly for complex mathematical tasks, is highly vulnerable to hardware noise and degrades significantly as noise levels increase. Furthermore, this noise causes an exponential increase in output tokens, leading to severe energy consumption that can nullify the primary efficiency advantages of the memristor. Therefore, we systematically appraise three training-free mitigation

strategies and summarize corresponding guidelines. Based on the observations, we further propose a practical strategy shallow (4×) that selectively repeats the first quarter of the model layers. Extensive experiments on more LLMs demonstrate that this approach achieves an excellent trade-off. Our findings offer valuable insights and practical guidelines for the robust deployment of LLMs on next-generation CIM hardware.

References

- [1] Josh Achiam, Steven Adler, Sandhini Agarwal, Lama Ahmad, Ilge Akkaya, Florencia Leoni Aleman, Diogo Almeida, Janko Altmenschmidt, Sam Altman, Shyamal Anadkat, et al. 2023. Gpt-4 technical report. *arXiv preprint arXiv:2303.08774* (2023).
- [2] Janice Ahn, Rishu Verma, Renze Lou, Di Liu, Rui Zhang, and Wenpeng Yin. 2024. Large Language Models for Mathematical Reasoning: Progresses and Challenges. In *Proc. 18th Conf. of the European Chapter of the ACL (EACL) Student Research Workshop*, Neele Falk, Sara Papi, and Mike Zhang (Eds.). Association for Computational Linguistics, St. Julian's, Malta, 225–237. doi:10.18653/v1/2024.eacl-srw.17
- [3] Michael Ahn, Anthony Brohan, Noah Brown, Yevgen Chebotar, Omar Cortes, Byron David, Chelsea Finn, Chuyuan Fu, Keerthana Gopalakrishnan, Karol Hausman, et al. 2022. Do as i can, not as i say: Grounding language in robotic affordances. In *Proc. Conf. on Robot Learning (CoRL)*. *arXiv preprint arXiv:2204.01691*.
- [4] Keivan Alizadeh, Seyed Iman Mirzadeh, Dmitry Belenko, S Khatamifard, Minsik Cho, Carlo C Del Mundo, Mohammad Rastegari, and Mehrdad Farajtabar. 2024. Llm in a flash: Efficient large language model inference with limited memory. In *Proc. 62nd Annual Meeting of the Association for Computational Linguistics (ACL)*. 12562–12584.
- [5] Mayank Arya and Yogesh Simmhan. 2025. Understanding the Performance and Power of LLM Inferencing on Edge Accelerators. *arXiv preprint arXiv:2506.09554* (2025).
- [6] Maciej Besta, Nils Blach, Ales Kubicek, Robert Gerstenberger, Michal Podstawski, Lukas Gianinazzi, Joanna Gajda, Tomasz Lehmann, Hubert Niewiadomski, Piotr Nyczyk, et al. 2024. Graph of thoughts: Solving elaborate problems with large language models. In *Proc. AAAI Conf. on Artificial Intelligence (AAAI)*, Vol. 38. 17682–17690.
- [7] Arjun Chaudhuri, Jonti Talukdar, Fei Su, and Krishnendu Chakrabarty. 2022. Functional criticality analysis of structural faults in AI accelerators. *IEEE Trans. Comput.-Aided Des. Integr. Circuits Syst.* 41, 12 (2022), 5657–5670.
- [8] An Chen and Ming-Ren Lin. 2011. Variability of resistive switching memories and its impact on crossbar array performance. In *Proc. Int'l Reliability Physics Symp. (IRPS)*. IEEE, MY–7.
- [9] Yu-Der Chih, Po-Hao Lee, Hidehiro Fujiwara, Yi-Chun Shih, Chia-Fu Lee, Rawan Naous, Yu-Lin Chen, Chieh-Pu Lo, Cheng-Han Lu, Haruki Mori, Wei-Chang Zhao, Dar Sun, Mahmud E. Sinangil, Yen-Huei Chen, Tan-Li Chou, Kerem Akarvardar, Hung-Jen Liao, Yih Wang, Meng-Fan Chang, and Tsung-Yung Jonathan Chang. 2021. 16.4 An 89TOPS/W and 16.3TOPS/mm² All-Digital SRAM-Based Full-Precision Compute-In Memory Macro in 22nm for Machine-Learning Edge Applications. In *Proc. IEEE Int'l Solid-State Circuits Conf. (ISSCC)*, Vol. 64. 252–254. doi:10.1109/ISSCC42613.2021.9365766
- [10] OpenCompass Contributors. 2023. OpenCompass: A Universal Evaluation Platform for Foundation Models. <https://github.com/open-compass/opencompass>.
- [11] Qingxiu Dong, Lei Li, Damai Dai, Ce Zheng, Jingyuan Ma, Rui Li, Heming Xia, Jingjing Xu, Zhiyong Wu, Baobao Chang, et al. 2024. A survey on in-context learning. In *Proc. Conf. on Empirical Methods in Natural Language Processing (EMNLP)*. 1107–1128.
- [12] Abhimanyu Dubey, Abhinav Jauhri, Abhinav Pandey, Abhishek Kadian, Ahmad Al-Dahle, Aiesha Letman, Akhil Mathur, Alan Schelten, Amy Yang, Angela Fan, et al. 2024. The llama 3 herd of models. *arXiv preprint arXiv:2407.21783* (2024).
- [13] Sicheng Feng, Gongfan Fang, Xinyin Ma, and Xinchao Wang. 2025. Efficient reasoning models: A survey. *arXiv preprint arXiv:2504.10903* (2025).
- [14] Mohamed Amine Ferrag, Norbert Tihanyi, and Merouane Debbah. 2025. From llm reasoning to autonomous ai agents: A comprehensive review. *arXiv preprint arXiv:2504.19678* (2025).
- [15] Daya Guo, Dejian Yang, Haowei Zhang, Junxiao Song, Ruoyu Zhang, Runxin Xu, Qihao Zhu, Shirong Ma, Peiyi Wang, Xiao Bi, et al. 2025. Deepseek-r1: Incentivizing reasoning capability in llms via reinforcement learning. *arXiv preprint arXiv:2501.12948* (2025).
- [16] Yuanbo Guo, Zheyu Yan, Xiaoting Yu, Qingpeng Kong, Joy Xie, Kevin Luo, Dewen Zeng, Yawen Wu, Zhengze Jia, and Yiyu Shi. 2024. Hardware design and the fairness of a neural network. *Nature Electronics* 7, 8 (2024), 714–723.
- [17] David Ha and Jürgen Schmidhuber. 2018. World models. *arXiv preprint arXiv:1803.10122* 2, 3 (2018).
- [18] Dan Hendrycks, Collin Burns, Saurav Kadavath, Akul Arora, Steven Basart, Eric Tang, Dawn Song, and Jacob Steinhardt. 2021. Measuring mathematical problem solving with the math dataset. *arXiv preprint arXiv:2103.03874* (2021).
- [19] Dovydas Joksas, Pedro Freitas, Zheng Chai, Wing H Ng, Mark Buckwell, C Li, WD Zhang, Q Xia, AJ Kenyon, and A Mehonic. 2020. Committee machines—a universal method to deal with non-idealities in memristor-based neural networks. *Nat. Commun.* 11, 1 (2020), 4273.
- [20] Benjamin Kubwimana and Qijing Huang. 2025. EdgeReasoning: Characterizing Reasoning LLM Deployment on Edge GPUs. *arXiv preprint arXiv:2511.01866* (2025).
- [21] Jinhao Li, Jiaming Xu, Shan Huang, Yonghua Chen, Wen Li, Jun Liu, Yaouxu Lian, Jiayi Pan, Li Ding, Hao Zhou, et al. 2024. Large language model inference acceleration: A comprehensive hardware perspective. *arXiv preprint arXiv:2410.04466* (2024).
- [22] Hunter Lightman, Vineet Kosaraju, Yuri Burda, Harrison Edwards, Bowen Baker, Teddy Lee, Jan Leike, John Schulman, Ilya Sutskever, and Karl Cobbe. 2023. Let's verify step by step. In *Proc. 12th Int'l Conf. on Learning Representations (ICLR)*.
- [23] Zhengwu Liu, Jie Mei, Jianshi Tang, Minpeng Xu, Bin Gao, Kun Wang, Sanchuan Ding, Qi Liu, Qi Qin, Weize Chen, et al. 2025. A memristor-based adaptive neuromorphic decoder for brain-computer interfaces. *Nature Electronics* (2025), 1–11.
- [24] Xiaochen Peng, Shanshi Huang, Yandong Luo, Xiaoyu Sun, and Shimeng Yu. 2019. DNN+NeuroSim: An End-to-End Benchmarking Framework for Compute-in-Memory Accelerators with Versatile Device Technologies. In *Proc. IEEE Int'l Electron Devices Meeting (IEDM)*. 32.5.1–32.5.4. doi:10.1109/IEDM19573.2019.8993491
- [25] David Rein, Betty Li Hou, Asa Cooper Stickland, Jackson Petty, Richard Yuanzhe Pang, Julien Dirani, Julian Michael, and Samuel R Bowman. 2024. Gpqa: A graduate-level google-proof q&a benchmark. In *Proc. 1st Conf. on Language Modeling (CoLM)*.
- [26] Chang Eun Song, Priansh Bhatnagar, Zihan Xia, Nam Sung Kim, Tajana S Rosing, and Mingyu Kang. 2025. Hybrid SLC-MLC RRAM Mixed-Signal Processing-in-Memory Architecture for Transformer Acceleration via Gradient Redistribution. In *Proc. 52nd Annual Int'l Symp. on Computer Architecture (ISCA)*. 1155–1170.
- [27] Fengbin Tu, Zihan Wu, Yiqi Wang, Ling Liang, Liu Liu, Yufei Ding, Leibo Liu, Shaojun Wei, Yuan Xie, and Shouyi Yin. 2022. A 28nm 15.59μJ/Token Full-Digital Bitline-Transpose CIM-Based Sparse Transformer Accelerator with Pipeline/Parallel Reconfigurable Modes. In *Proc. IEEE Int'l Solid-State Circuits Conf. (ISSCC)*, Vol. 65. 466–468. doi:10.1109/ISSCC42614.2022.9731645
- [28] Deepak Vungarala, Md Hasibul Amin, Pietro Mercati, Arnob Ghosh, Arman Roohi, Ramtin Zand, and Shaahin Angizi. 2025. LIMCA: LLM for Automating Analog In-Memory Computing Architecture Design Exploration. *arXiv preprint arXiv:2503.13301* (2025).
- [29] Rui Wang, Hongru Wang, Boyang Xue, Jianhui Pang, Shudong Liu, Yi Chen, Jiahao Qiu, Derek Fai Wong, Heng Ji, and Kam-Fai Wong. 2025. Harnessing the reasoning economy: A survey of efficient reasoning for large language models. *arXiv preprint arXiv:2503.24377* (2025).
- [30] Zhehui Wang, Tao Luo, Cheng Liu, Weichen Liu, Rick Siow Mong Goh, and Weng-Fai Wong. 2024. Enabling energy-efficient deployment of large language models on memristor crossbar: A synergy of large and small. *IEEE Trans. Pattern Anal. Mach. Intell. (TPAMI)* (2024).
- [31] Jason Wei, Xuezhi Wang, Dale Schuurmans, Maarten Bosma, Fei Xia, Ed Chi, Quoc V Le, Denny Zhou, et al. 2022. Chain-of-thought prompting elicits reasoning in large language models. *Adv. Neural Inf. Process. Syst. (NeurIPS)* 35 (2022), 24824–24837.
- [32] Taiqiang Wu, Chenchen Ding, Wenying Zhou, Yuxin Cheng, Xincheng Feng, Shuqi Wang, Chufan Shi, Zhengwu Liu, and Ngai Wong. 2025. HaLoRA: Hardware-aware Low-Rank Adaptation for Large Language Models Based on Hybrid Compute-in-Memory Architecture. *arXiv preprint arXiv:2502.19747* (2025).
- [33] Taiqiang Wu, Runming Yang, Tao Liu, Jiahao Wang, and Ngai Wong. 2025. Revisiting Model Interpolation for Efficient Reasoning. *arXiv preprint arXiv:2510.10977* (2025).
- [34] Lixue Xia, Wenqin Huangfu, Tianqi Tang, Xiling Yin, Krishnendu Chakrabarty, Yuan Xie, Yu Wang, and Huazhong Yang. 2017. Stuck-at fault tolerance in RRAM computing systems. *IEEE J. Emerg. Sel. Topics Circuits Syst.* 8, 1 (2017), 102–115.
- [35] An Yang, Anfeng Li, Baosong Yang, Beichen Zhang, Binyuan Hui, Bo Zheng, Bowen Yu, Chang Gao, Chengen Huang, Chenxu Lv, et al. 2025. Qwen3 technical report. *arXiv preprint arXiv:2505.09388* (2025).
- [36] Peng Yao, Huaqiang Wu, Bin Gao, Jianshi Tang, Qingtian Zhang, Wenqiang Zhang, Joshua Yang, and He Qian. 2020. Fully hardware-implemented memristor convolutional neural network. *Nature* 577, 7792 (2020), 641–646.
- [37] Tao Yu, Rui Zhang, Kai Yang, Michihiro Yasunaga, Dongxu Wang, Zifan Li, James Ma, Irene Li, Qingning Yao, et al. 2018. Spider: A large-scale human-labeled dataset for complex and cross-domain semantic parsing and text-to-sql task. In *Association for Computational Linguistics (ACL)*. *arXiv preprint arXiv:1809.08887*.
- [38] Wenqiang Zhang, Xiaochen Peng, Huaqiang Wu, Bin Gao, Hu He, Youhui Zhang, Shimeng Yu, and He Qian. 2019. Design guidelines of RRAM based neural-processing-unit: A joint device-circuit-algorithm analysis. In *Proc. 56th Annual*

Design Automation Conf. (DAC). 1–6.

- [39] Jeffrey Zhou, Tianjian Lu, Swaroop Mishra, Siddhartha Brahma, Sujoy Basu, Yi Luan, Denny Zhou, and Le Hou. 2023. Instruction-following evaluation for large

language models. *arXiv preprint arXiv:2311.07911* (2023).